Journal of Organometallic Chemistry 696 (2011) 3785–3791

Contents lists available at SciVerse ScienceDirect

Journal of Organometallic Chemistry

journal homepage: www.elsevier.com/locate/jorganchem

Synthesis, characterization and structure–property relationship studies of cobaloximes with dithienylglyoxime as the equatorial ligand

Kamlesh Kumar*, Bhagwan D. Gupta[1]

Department of Chemistry, Indian Institute of Technology, Kanpur 208 016, India

ARTICLE INFO

Article history:
Received 30 July 2011
Received in revised form
24 August 2011
Accepted 25 August 2011

Keywords:
Dithienylglyoxime
Cobaloxime
Cis–trans influence
Oxygen insertion
Electrochemistry
Structure elucidation

ABSTRACT

The synthesis of cobaloximes, X/RCo(dThgH)$_2$Py (X = Cl, R = Me, Et, *n*-Pr, *n*-Bu and Bn) has been described. All the complexes have been characterized by elemental analyses and NMR spectral studies. The molecular structures of ClCo(dThgH)$_2$Py, MeCo(dThgH)$_2$Py, EtCo(dThgH)$_2$Py and BnCo(dThgH)$_2$Py complexes are determined by X-ray crystallography. The electron withdrawing nature of 2-thienyl ring affects the NMR as well as electrochemical behavior of these complexes. The electrochemical reduction from Co(III) to Co(II) and from Co(II) to Co(I) are much easier in ClCo(dThgH)$_2$Py as compared to chlorocobaloximes with the other dioximes (gH, dmgH, dpgH, dmestgH). The molecular oxygen insertion in the Co–C bond of benzyl complex (**6**) has been examined and a comparison of its reaction rate with other similar cobaloximes is discussed. The structural features of a dioxy complex Bn(O$_2$)Co(dThgH)$_2$Py (**7**) have also been reported.

1. Introduction

The spectral and structural properties of organocobaloximes[2] have been extensively studied and reviewed [1–5] over the past four decades ever since these have been proposed as structural and functional model of vitamin B$_{12}$ by G. N. Schrauzer [6–8]. These complexes have established an independent research field by itself due to their use as catalysts in chemical reactions [9,10] and as templates in organic syntheses [11–19]. However, the main interest remains in their role as models of vitamin B$_{12}$ coenzyme because the studies with cobaloximes have helped to understand the chemistry and biochemistry of B$_{12}$ coenzyme [20–22].

It is well known that cleavage of Co–C bond is a necessary step in B$_{12}$-dependent enzymatic as well as cobaloxime-mediated reactions [1,3,11–19]. The weakening of Co–C bond in organocobaloximes has been interpreted as a function of steric as well as electronic properties of R, L, and B ligands [1–3,23,24].

The recent works on organocobaloximes with different dioximes have shown that the effect of dioxime on the Co–C bond (*cis* influence) far exceeds the *trans* influence of the axial base [25–32]. A slight variation in equatorial ligand results in significant change in Co–C bond stability/reactivity as well as NMR chemical shifts. Hence, there has been considerable interest in the synthesis and structural characterization of organocobaloximes with modified equatorial dioxime and also study the structure–property relationship in these complexes.

Keeping the above in view, we have synthesized and characterized a series of X/RCo(dThgH)$_2$Py (X = Cl, R = Me, Et, *n*-Pr, *n*-Bu and Bn, **1**–**6**) with dithienylglyoxime (dThgH) as an equatorial ligand (Scheme 1). All these complexes are new and have been reported for the first time. The molecular structures of **1**, **2**, **3** and **6** have been determined by X-ray crystallography. In addition, we have also studied Co–C bond reactivity in benzyl complex (**6**) with molecular oxygen under photolytic condition. The insertion of molecular oxygen in Co–C bond of complex **6** has resulted in the dioxy complex, Bn(O$_2$)Co(dThgH)$_2$Py (**7**). The structural features of oxygen inserted cobaloxime (**7**) are also reported.

2. Results and discussion

2.1. Synthesis of dithienylglyoxime and cobaloximes (*1*–*7*)

Dithienylglyoxime (dThgH$_2$) was synthesized from (2-thienyl) MgBr and dichloroglyoxime following the procedure developed for

* Corresponding author. Tel.: +91 512 2597730; fax: +91 512 2597436.
E-mail address: kamlesh@iitk.ac.in (K. Kumar).

[1] Prof. Bhagwan D. Gupta deceased on 31 March 2011.

[2] Organocobaloximes have the general formula RCo(L)$_2$B, where R is an organic group *σ*-bonded to cobalt. B is an axial base trans to the organic group and L is a monoanionic dioxime e.g. glyoxime (gH), dimethylglyoxime (dmgH), 1,2-cyclohexanedione dioxime (chgH), diphenylglyoxime (dpgH), dimesitylglyoxime (dmestgH), bis(thiophenyl)glyoxime (dSPhgH) and bis(phenylselanyl)glyoxime (dSePhgH).

0022-328X/$ – see front matter © 2011 Elsevier B.V. All rights reserved.
doi:10.1016/j.jorganchem.2011.08.035

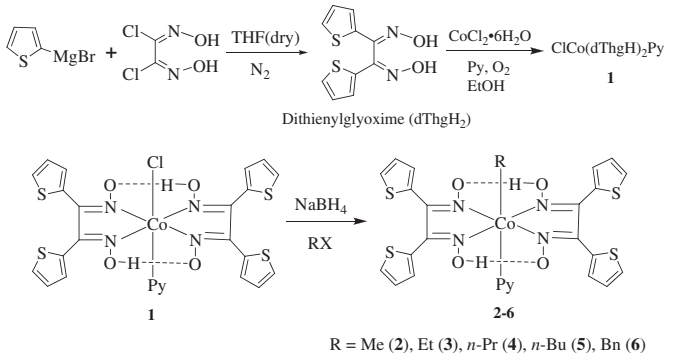

Scheme 1. Synthesis of dithienylglyoxime ($dThgH_2$) and cobaloximes (**1**–**6**).

$dmestgH_2$ [33]. The synthetic route is shown in Scheme 1. The 2-thienyl group displaced the chloride of dichloroglyoxime and gave the desired dithienylglyoxime product. The synthesis of $ClCo(dThgH)_2Py$ (**1**) was accomplished by refluxing a stoichiometric mixture of $CoCl_2 \cdot 6H_2O$, $dThgH_2$ and pyridine in ethanol/THF solvent mixture followed by the aerial oxidation. We found that the synthesis of **1** in ethanol/THF solvent mixture (1:1) gave better yield (70%) than in ethanol only (30%). The complexes **2**–**6** were prepared by oxidative alkylation of cobaloxime(I) anion generated *in situ* by $NaBH_4$ reduction of $ClCo(dThgH)_2Py$ in CH_3OH. The reaction of molecular oxygen with benzyl cobaloxime (**6**) in CH_2Cl_2 at 0 °C under visible light proceeds smoothly and the dioxy cobaloxime (**7**) is formed in good yield within 1 h.

2.2. NMR spectral studies (^1H and ^{13}C)

^1H and ^{13}C NMR data for all complexes (**1**–**7**) and $dThgH_2$ are summarized in experimental section. The solubility of free ligand $dThgH_2$ is poor in $CDCl_3$ and hence a few drops of DMSO-d_6 are necessary to record the NMR. The ^1H NMR spectra of the complexes are easily assigned on the basis of the chemical shifts, their relative intensities and also assignments are consistent with the previously described complexes [25,26,29].

The Co–C bond stability in organocobaloximes depends on both the *cis* and *trans* influences. The *cis* influence study has gained importance only recently [25–32,34–36]. Usually, to study the *cis* influence, either the axial ligands R/X or base B is varied, keeping the same dioxime, or the dioxime is varied, keeping the axial ligands constant and changes are monitored spectroscopically. The NMR studies of cobaloximes with different dioximes have shown that the chemical shifts of Py_α, C=N and the α-carbon bound to cobalt are most affected.

The extent of electron density on the metallabicycle for different dioximes (keeping R/X and Py constant) can be understood by comparing the coordination shift, $\Delta\delta(^{13}C_{C=N})$ values [37]. In general, $\delta^{13}C_{C=N}$ in free dioxime is shifted upfield on coordination to cobalt. We find that the $\delta^{13}C_{C=N}$ signals in dThgH complexes (**1**–**6**) appeared significantly downfield as compared to the values in cobaloximes with other dioximes. The order based on the upfield shift value is gH > dmgH > dpgH > chgH > dmestgH > dThgH (Table S1). This suggests the charge density on C=N is much lower in dThgH complexes than the other dioxime complexes. The electrochemical study also shows up this effect (see later). The charge density on C=N should also affect the chemical shifts for O–H···O proton signals. The lower the charge density on C=N, weaker the hydrogen bond and hence a more downfield shift of O–H···O resonance would be expected. Indeed a considerable downfield shift of O–H···O signals is observed in **1**–**6** as compared to the complexes with other dioximes and follows the order dThgH > dmestgH > dpgH > dmgH (Table S2).

The chemical shift of Py_α protons is affected not only by the *trans* effect of the R/X group but also by the ring current in the metallabicycle. The Py_α shows a downfield shift of 0.07–0.14 ppm in **2**–**6** and an upfield shift of 0.14 ppm in **1** as compared to the unligated pyridine (Table S3). This is due to the *trans* effect that works differently in inorganic and organic cobaloximes as shown recently [38]. The *cis* influence of the dioxime ligand on pyridine is observed by comparing the coordination shift of pyridine protons ($\Delta\delta^1H$), keeping the same R/X but changing the equatorial ligand. A comparison of the $\Delta\delta^1H(Py_\alpha)$ values in **1**–**6** with the values in other cobaloximes, $RCo(dioxime)_2Py$, gives the order dmestgH > dpgH > dThgH > gH ≈ dmgH ≈ chgH (Table S3).

Since the chemical shift of the axial Co–C_α protons ($CoCH_3$ protons in **2** and $CoCH_2$ protons in **3**–**6**) depends on the *cis* influence of the dioxime moiety and the ring current in the dioxime moiety, the Co–C_α protons in complexes **2**–**6** appear downfield from the corresponding dmgH complexes and this downfield shift is comparable with the dpgH and dmestgH complexes (Table S4).

The chemical shift values of CH_2, Py_α and the dioxime (C=N) are further affected in the dioxy complex **7**. The signal for CH_2O_2 is shifted downfield by 0.97 ppm in ^1H NMR and 43.67 ppm in ^{13}C NMR as compared to precursor complex **6**. The Py_α protons are shifted upfield (0.19 ppm) whereas $^{13}C(Py_\alpha)$ and $^{13}C_{C=N}$ signals are appeared downfield by 0.88 and 2.0 ppm, respectively as compared to **6**.

2.3. Electrochemical studies (cyclic voltammetry)

The electrochemical behavior of **1**, **3** and **6** has been studied to understand the effect of dioxime (dThgH) on the redox potentials of the cobalt center. The cyclic voltammograms are shown in Figs. 1 and 2, and the CV data are given in Table 1. Three types of redox couple; Co(III)/Co(II), Co(II)/Co(I) and Co(IV)/Co(III) in the cyclic voltammogram are expected in any cobaloxime but complexes that describe entire redox processes are very few [39–42].

The cyclic voltammogram of **1** (Fig. 1) shows one irreversible peak at −0.239 V and one quasi-reversible peak ($E_{1/2}$ = −0.643 V) in the reductive half corresponding to Co(III)/Co(II) and Co(II)/Co(I), respectively. In the oxidation half only one quasi-reversible wave corresponding to Co(IV)/Co(III) ($E_{1/2}$ = 1.368 V) is observed. The

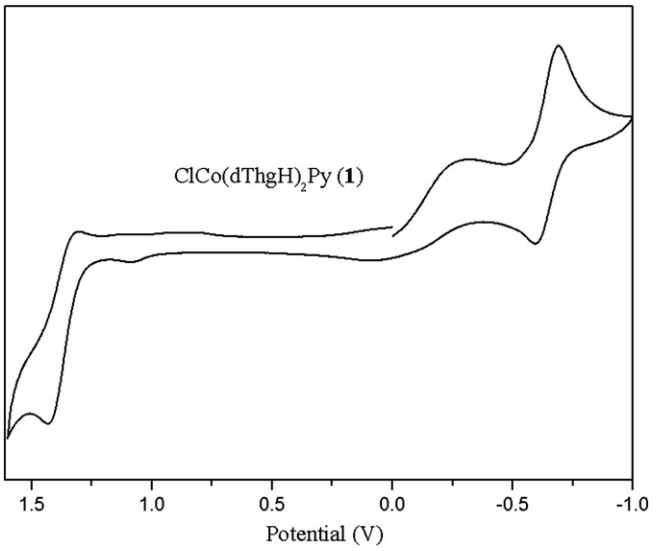

Fig. 1. Cyclic voltammogram of 1 in CH_2Cl_2 with 0.1 M $^nBu_4NPF_6$ as supporting electrolyte at 0.1 V/s at 25 °C.

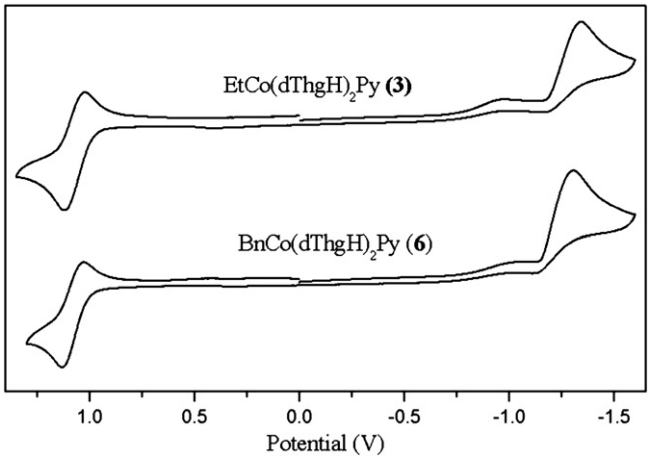

Fig. 2. Cyclic voltammograms of **3** and **6** in CH_2Cl_2 with 0.1 M $^nBu_4NPF_6$ as supporting electrolyte at 0.1 V/s at 25 °C.

values show that **1** is the most easily reduced of the chloroocobaloximes with dioxime having carbon side chain (Table S5). It points to the electron withdrawing effect imparted by the 2-thienyl ring which results in lower electron density on the cobalt center of complex **1**. The NMR studies also gave the same information.

The cyclic voltammograms of the organocobaloximes **3** and **6** (Fig. 2) show only one irreversible reduction response corresponding to Co(III)/Co(II) at −1.341 and −1.302 V, respectively. In the oxidative half a quasi-reversible one-electron oxidation wave corresponding to Co(IV)/Co(III) is observed. The $E_{1/2}$ value for this process is 1.069 and 1.079 V in complexes **3** and **6**, respectively. Due to the higher σ donation ability of the alkyl groups, the Co(III)/Co(II) redox process in **3** and **6** is considerably cathodically shifted and hence the Co(II)/Co(I) response is further cathodically shifted and is not observed even down to −1.6 V.

2.4. Molecular structures of *1*, *2*, *3* and *6*

Molecular structures of the complexes **1**, **2**, **3** and **6** have been determined by X-ray crystallography. Selected bond lengths and bond angles are given in Table 2 and molecular structures with selected numbering schemes are depicted in Figs. 3–6. In all the structures, cobalt atom has a distorted octahedral geometry with four N atoms of the dioxime (dThgH) in the equatorial plane and the axial positions are occupied by R/X and pyridine.

The $Co(dThgH)_2$ unit in cobaloximes undergoes geometrical deformations, due to flexibility, which is roughly represented by the displacement of cobalt out of 4-nitrogen plane (d) and by the butterfly bending angle between two dioxime units (α). The positive value of α and d indicates bending toward R/X and displacement toward base and *vice versa*. The deviations of cobalt atom from mean equatorial N_4 plane (d) are +0.0444(5), +0.0385(3), +0.0436(3) and +0.0107(5) Å in **1**, **2**, **3** and **6**, respectively. The deviation is small and is toward the base, pyridine. Since bending angle (α) is a measure of interaction between the axial and equatorial ligand, a high α value for **6** (−7.57°) as compared to **1**, **2** and **3** (1.08, 2.84, and 1.68°, respectively) is quite justified because of C–H···π interaction. The Co–Cl or Co–C bond distances [2.222(1), 1.992(1), 2.025(1), 2.062(3) Å] and Co–N_{py} bond distances [1.955(3), 2.065(1), 2.048(1), 2.063(3) Å] in **1**, **2**, **3** and **6** do not differ significantly from the reported values for the corresponding X/RCo(dioxime)$_2$Py complexes (Tables S6 and S7). However, the Co–C bond distance increases from 1.992(1) Å in **2** to 2.025(1) Å in **3** and 2.062(3) Å in **6** with increasing bulk of axial alkyl/benzyl group. The benzyl group in complex **6** is located over the dioxime wing and shows $\pi\cdots\pi$ and C–H···π interactions with the dioxime moiety. The distances of $\pi_{dioxime}\cdots\pi_{benzyl}$ and C8–H8···π_{benzyl} are 3.586(1) and 3.702(1) Å, respectively (Fig. 6).

2.5. Molecular structure of Bn(O_2)Co(dThgH)$_2$Py (*7*)

A slow evaporation of solvent from the solution of **7** (CH_3OH/$CHCl_3$) has resulted in the formation of brown crystals. The X-ray data analysis of **7** shows two molecules in its asymmetric unit and they are numbered as **7A** and **7B**. The molecular structure with selected numbering scheme is shown in Fig. 7 and the selected bond lengths, bond angles and other structural parameters are given in Table 3. The Co–O_{ax}, Co–N_{py} and O–O mean bond distances; 1.878(1), 1.992(2) and 1.451(2) Å respectively, are similar to those in the reported peroxo cobaloximes [32,43–46]. In both molecules the displacement of Co atom (d) from N_4 plane is toward pyridine and bending of dioxime units (α) is toward the BnO_2. It is interesting to note that the bending of dioxime units in oxygen inserted complex, Bn(O_2)Co(dThgH)$_2$Py is opposite to the precursor benzyl cobaloxime (**6**) which indicates the steric interaction of axial benzyl with equatorial dioxime decreased after oxygen insertion. The orientation of benzyl groups in both molecules of **7** in asymmetric unit is different and angles of pyridine plane with benzyl ring plane are 55.7° and 78.6°, respectively in **7A** and **7B**. In the crystal packing diagram, molecules of **7** exhibit weak intermolecular C–H···O interactions (C22A–H22A···O6A = 2.585(2) Å in **7A** and C24B–H24B···O6B = 2.485(2) Å in **7B**) leading to one-dimensional polymeric chains of **7A** and **7B**. Such 1-D chains of **7A** and **7B** are interconnected through $\pi\cdots\pi$ interactions between the 2-thienyl rings of dioximes with a distance of 3.714(1) Å between the centroids of stacked rings; resulting 1-D double-chain polymeric network (Fig. S1).

2.6. Kinetic study of oxygen insertion in the Co–C bond of complex *6*

The molecular oxygen insertion into the Co–C bond has extensively been used to test the reactivity of organocobaloximes [26,32,43–53]. Since the homolysis of Co–C bond is the key step in this reaction and the effect of equatorial dioxime (*cis* influence) is felt most on the Co–C bond, both are related to each other and

Table 1
CV Data for complexes **1**, **3** and **6** in CH_2Cl_2 and $^nBu_4NPF_6$ at 0.1 V/s at 25 °C.

No	Co(III)/Co(II)			Co(II)/Co(I)				Co(IV)/Co(III)			
	E_{pc}[a] (V)	E_{pc}[b] (V)	i_{pc} (μA)	$E_{1/2}$(V)[a] (ΔE_p, mV)	$E_{1/2}$[b] (V)	i_{pc} (μA)	i_{pa} (μA)	$E_{1/2}$(V)[a] (ΔE_p, mV)	$E_{1/2}$[b] (V)	i_{pc}	i_{pa}
1	−0.239	−0.666	2.01	−0.643(95)	−1.069	3.45	2.91	1.368 (128)	0.941	2.68	7.11
3	−1.341	−1.768	6.71					1.069 (95)	0.642	4.02	7.22
6	−1.302	−1.729	7.38					1.079 (106)	0.652	3.32	6.62

[a] *Vs.* Ag/AgCl.
[b] *Vs.* Fc/Fc^+ ($E_{1/2}$ = 0.4269 V).

Table 2
Selected bond lengths and bond angles for **1**, **2**, **3** and **6**.

Parameters	1	2	3	6
Co–C/Cl (Å)	2.222(1)	1.992(1)	2.025(1)	2.062(3)
Co–N_{py} (Å)	1.955(3)	2.065(1)	2.048(1)	2.063(3)
α (°)	+1.08	−2.84	−1.68	−7.57
d (Å)	+0.0444(5)	+0.0385(3)	+0.0436(3)	+0.0107(5)
τ (°)	85.73(10)	68.14(32)	87.44(10)	89.06(35)

follow the same order in benzyl complexes [26,30–32,43]. Therefore, we have undertaken the study of Co–C bond reactivity in complex **6**. The inherently weak Co–C bond and also the weak interaction of benzyl group with the equatorial dioxime in benzyl complex (**6**) make it an ideal system for such study. The rate study is carried out following the procedure reported in earlier studies under pseudo-first-order conditions at 0 °C [31,32]. The λ_{max} for the Co–C CT band in benzyl cobaloxime (**6**) is 454 nm. The rate constant (k_{obs}) is calculated from the slope of the linear plot of $\ln(A_t - A_\infty)$ *versus* time, where A_t is the absorbance at time t and A_∞ is the final absorbance, and is given in Fig. 8. The rate data in Table 4 shows that the oxygen insertion depends upon the dioxime and follows the order dmestgH > dThgH > dpgH > dmgH. Interestingly, the rate of oxygen insertion in dThgH complex (**6**) is faster than that of the dpgH complex although the *cis* influence in dpgH and dThgH complexes is quite similar on the basis of the chemical shift value for Co–CH_2 protons and also the Co–C bond distances are similar in both complexes (Table S7). The larger puckering of the Co(dioxime)$_2$ unit in complex **6** ($\alpha = -7.57°$ and $d = +0.0107$ Å) as compared to the BnCo(dpgH)$_2$Py ($\alpha = 1.75°$ and $d = -0.0275$ Å) [54] might be the driving force for the higher rate constant in BnCo(dThgH)$_2$Py.

3. Conclusion

In this work we have described synthesis and characterization of cobaloximes with dithienylglyoxime as the equatorial ligand. The electron withdrawing nature of 2-thienyl ring affects the NMR as well as the electrochemical behavior of these complexes. The $^{13}C_{C=N}$ signals in dThgH complexes appear significantly downfield as compared to cobaloximes with other dioxime systems. Among all the reported chlorocobaloximes, ClCo(dThgH)$_2$Py (**1**) is most easy to reduce electrochemically from Co(III) to Co(II) and Co(II) to Co(I). The reactivity of benzyl complex with molecular oxygen under photolytic condition has been examined and a comparison of its reaction rate with the other similar cobaloximes gives the order of equatorial dioximes, dmestgH > dThgH > dpgH > dmgH.

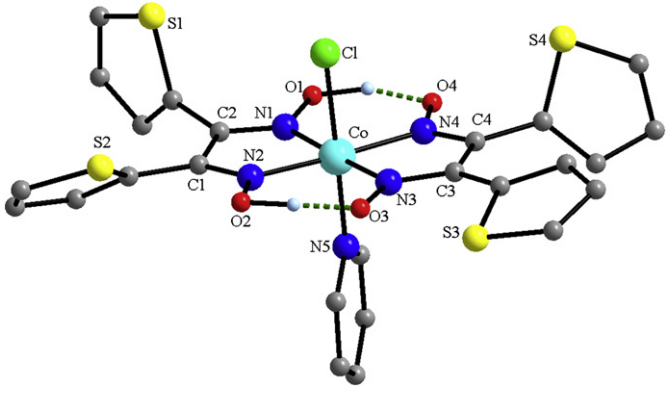

Fig. 3. Molecular structure of ClCo(dThgH)$_2$Py (**1**). Solvent molecule and most of the hydrogen atoms have been omitted for clarity.

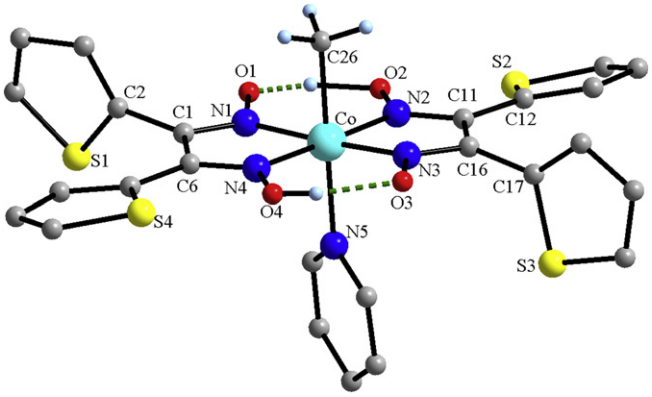

Fig. 4. Molecular structure of MeCo(dThgH)$_2$Py (**2**). Most of the hydrogen atoms have been omitted for clarity.

4. Experimental section

4.1. Materials and physical measurements

$CoCl_2 \cdot 6H_2O$ (SD Fine, India), 2-bromothiophene, iodomethane, iodoethane, 1-bromopropane, 1-bromobutane and benzyl chloride (all from Sigma-Aldrich, USA) were used as received without further purifications. Dichloroglyoxime was prepared and purified according to reported literature procedure [30]. The solvents were purified rigorously by standard procedures prior to their use and THF was dried over sodium/benzophenone. A Julabo UC-20 low-temperature refrigerated circulator was used to maintain the desired temperature. Cyclic voltammetry measurements were carried out using a BAS Epsilon electrochemical work station with a platinum working electrode, a Ag/AgCl reference electrode (3 M NaCl) and a platinum–wire counter electrode. All measurements were performed in 0.1 M $^nBu_4NPF_6$ in CH_2Cl_2 (dry) at a concentration of 1 mM of each complex. ^{1}H NMR spectra were recorded on JEOL JNM LAMBDA-400 model operating at 400 MHz and ^{13}C NMR spectra were recorded on JEOL ECX-500 model operating at 125 MHz in $CDCl_3$ with TMS as internal standard. Elemental analyses for C, H and N were performed on CE-440 Elemental Analyzer.

4.2. X-ray crystal structure determination and refinements

Single crystals suitable for X-ray crystallographic analyses were obtained by the slow evaporation of the solvent from the solutions of complexes [CH_3OH/CH_2Cl_2 for **1** and $CH_3OH/CHCl_3$ for **2**, **3**, **6** and

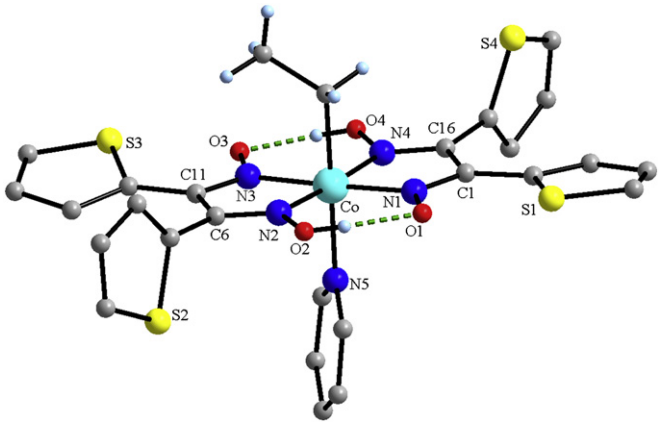

Fig. 5. Molecular structure of EtCo(dThgH)$_2$Py (**3**). Most of the hydrogen atoms have been omitted for clarity.

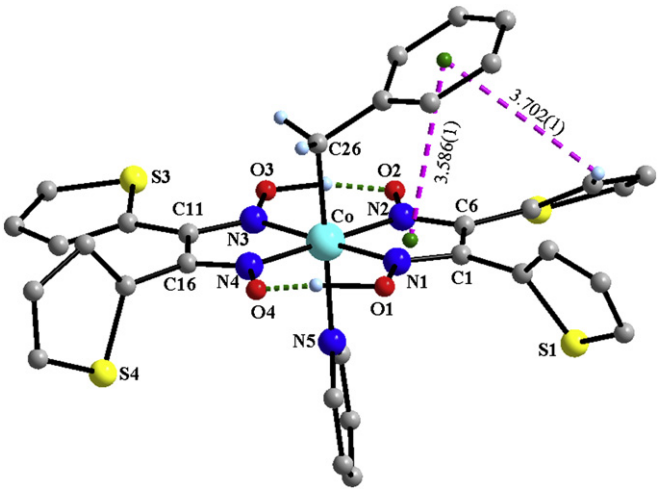

Fig. 6. Molecular structure of $BnCo(dThgH)_2Py$ (**6**). Most of the hydrogen atoms have been omitted for clarity.

7]. X-ray crystallographic data were collected using graphite-monochromated Mo *Kα* radiation (λ = 0.71073 Å) on "Bruker SMART APEX CCD diffractometer" at 100 K. The linear absorption coefficients, scattering factors for the atoms and the anomalous dispersion corrections were taken from the *International Tables for X-ray Crystallography* [55]. The program SMART [56] was used for collecting frames of data, indexing reflections, and determining lattice parameters. The data integration and reduction were processed with SAINT software [56]. An empirical absorption correction was applied to the collected reflections with SADABS [57] using XPREP [58]. All the structures were solved by the direct method using the program SHELXS-97 [59] and were refined on F^2 by the full-matrix least-squares technique using the SHELXL-97 [59] program package. All non-hydrogen atoms were refined with anisotropic displacement parameters in all the structures. The hydrogen atom positions or thermal parameters were not refined but were included in the structure factor calculations. The 2-thienyl rings in all complexes were found to be disordered and were modeled satisfactorily using part instructions. The pertinent crystal

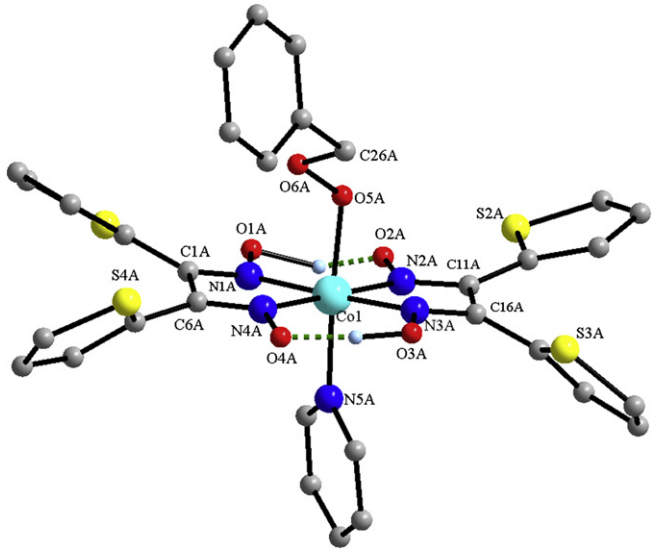

Fig. 7. Molecular structure of $BnO_2Co(dThgH)_2Py$ (**7**). One molecule of **7** present in the asymmetric unit, solvent molecules and most of the hydrogen atoms have been omitted for clarity.

Table 3
Selected bond lengths and bond angles for **7**.

Parameters	7	
	A	B
Co–O_{ax} (Å)	1.879 (1)	1.876 (1)
Co–N_{py} (Å)	1.990 (2)	1.994 (2)
O–O (Å)	1.454 (2)	1.447 (2)
O–C (Å)	1.436 (3)	1.444 (3)
Co–O–O (°)	113.92 (9)	116.98 (9)
O–O–C (°)	105.87 (11)	107.27 (13)
Co–O–O–C (°)	102.79 (13)	−105.53 (14)
O–C–C (°)	107.65 (15)	106.02 (17)
O–O–C–C (°)	−179.71 (15)	−163.30 (13)
N_{py}–Co–O_{ax} (°)	170.44 (6)	173.90 (5)
d (Å)	+0.0196 (4)	+0.0438 (4)
α (°)	+3.01	+7.43
τ (°)	70.44 (34)	75.78 (13)

data and refinement parameters for compounds **1**, **2**, **3**, **6** and **7** are compiled in Table 5.

4.3. Syntheses

4.3.1. Synthesis of dithienylglyoxime ($dThgH_2$)

A solution of dichloroglyoxime (1.0 g, 6.36 mmol) in 10 mL dry THF was added slowly with stirring to a solution of (2-thienyl)MgBr at 0 °C under nitrogen atmosphere. The (2-thienyl)MgBr was prepared in dry THF (25 mL) from 2-bromothiophene (5.198 g, 31.83 mmol), Mg (0.851 g, 35.01 mmol) and one crystal of I_2 under nitrogen atmosphere. After the addition of dichloroglyoxime, the solution was allowed to warm to room temperature and stirred further for 5 h before quenching with saturated aqueous NH_4Cl (20 mL). The content was stirred vigorously for 10 min. The two layers were separated and the aqueous layer was extracted with THF (3 × 7 mL). The combined organic solution washed with brine solution and dried over anhydrous Na_2SO_4. The solvent was evaporated off under reduced pressure on a rotary evaporator to result in a brown colored solid which was washed with petroleum ether. Yield: 1.437 g (~89%). ^1H NMR (400 MHz, $CDCl_3$ + DMSO-d_6, δ ppm): thienyl protons = 7.38 (2H, d, J = 5.2 Hz), 7.14 (2H, d, J = 3.8 Hz), 6.86–6.84 (2H, m), N–O···H = 11.70 (s). ^{13}C NMR (125 MHz, $CDCl_3$ + DMSO-d_6, δ ppm): 146.04 (C=N), 131.89, 130.93, 130.50, 125.63. Anal. Calcd. for $C_{10}H_8N_2O_2S_2$: C, 47.60; H, 3.20; N, 11.10. Found: C, 47.86; H, 3.11; N, 11.27.

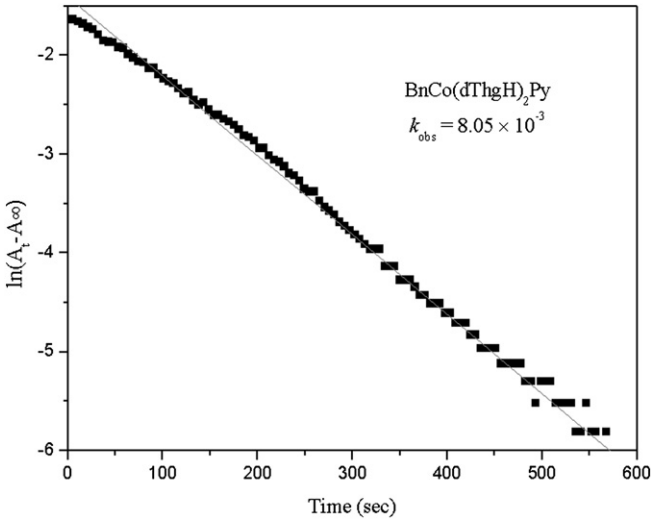

Fig. 8. Plot of $\ln(A_t - A_\infty)$ *versus* time (sec) for $BnCo(dThgH)_2Py$ (**6**).

Table 4
Pseudo-first-order rate constant (k_{obs}) for oxygen insertion in BnCo(dioxime)$_2$Py.

BnCo(dioxime)$_2$Py	k_{obs} (s^{-1})	Ref.
BnCo(dmgH)$_2$Py	1.2×10^{-3}	[32]
BnCo(dpgH)$_2$Py	4.8×10^{-3}	[32]
BnCo(dmestgH)$_2$Py	5.0×10^{-2}	[32]
BnCo(dThgH)$_2$Py	8.05×10^{-3}	this work

*4.3.2. Synthesis of ClCo(dThgH)$_2$Py (**1**)*

In a typical reaction, pyridine (0.2 mL, 2.5 mmol) was added to a hot solution of dithienylglyoxime (0.252 g, 1.0 mmol) and $CoCl_2 \cdot 6H_2O$ (0.118 g, 0.5 mmol) in 30 mL of 1:1 ethanol/THF solvent mixture and the resulting solution was refluxed for 1 h. The solution was cooled to room temperature and air was passed vigorously for 3 h with occasional swirling to get desired crude product. The solid crude product was filtered, washed with water and dried over P_2O_5 overnight and purified on a silica gel column using CH_2Cl_2. Yield: 0. 237 g (~70%). ^{1}H NMR (400 MHz, $CDCl_3$, δ ppm): Py_α = 8.43 (2H, d, J = 5.6 Hz), Py_β = 7.29 (2H, t, J = 7.2 Hz), Py_γ = 7.74 (1H, t, J = 7.4 Hz), thienyl protons = 7.56 (4H, d, J = 3.6 Hz), 7.03–7.00 (8H, m), 18.90 (2H, s, O–H···O). ^{13}C NMR (125 MHz, $CDCl_3$, δ ppm): 150.86 (Py_α), 147.09 (C=N, C_q), 139.27 (Py_γ), 130.94, 129.96, 129.40, 126.16, 126.03. Anal. Calcd. for $C_{25}H_{19}ClCoN_5O_4S_4$: C, 44.41; H, 2.83; N, 10.36. Found: C, 44.26; H, 2.71; N, 10.51.

*4.3.3. Synthesis of RCo(dThgH)$_2$Py (**2**–**6**): general procedure*

These complexes were synthesized by following the general procedure described earlier for the synthesis of RCo(dioxime)$_2$Py and involved the reaction of cobaloxime(I) with organic halide. In typical procedure, a solution of **1** (0.100 g, 0.147 mmol) in 10 mL of CH_3OH was purged thoroughly with N_2 for 20 min and was cooled to 0 °C with stirring. The solution turned deep blue after the addition of few drops of aqueous NaOH followed by $NaBH_4$ (0.012 g, 0.320 mmol in 0.5 mL of water). The color of the solution turned orange–red on the addition of organic halide (0.3 mmol). The reaction was stirred 1 h at 0 °C then poured into 20 mL chilled water containing few drops of pyridine. The resulting orange–red precipitate was filtered, washed with water, and dried. The crude product was purified on the silica gel column using CH_2Cl_2 as eluent.

*4.3.3.1. MeCo(dThgH)$_2$Py (**2**).* Yield: 0.052 g (~54%). ^{1}H NMR (400 MHz, $CDCl_3$, δ ppm): Py_α = 8.71 (2H, d, J = 5.2 Hz), Py_β = 7.37 (2H, t, J = 7.0 Hz), Py_γ = 7.76 (1H, t, J = 8.0 Hz), thienyl protons = 7.49 (4H, d, J = 5.2 Hz), 6.98 (4H, t, J = 4.4 Hz), 6.86 (4H, d, J = 3.6 Hz), 1.32 (3H, s, $CoCH_3$), 18.94 (2H, s, O–H···O). ^{13}C NMR (125 MHz, $CDCl_3$, δ ppm): 149.87 (Py_α), 144.57 (C=N, C_q), 138.01 (Py_γ), 130.34, 129.62, 128.51, 126.06, 125.76. Anal. Calcd. for $C_{26}H_{22}CoN_5O_4S_4$: C, 47.63; H, 3.38; N, 10.68. Found: C, 47.74; H, 3.45; N, 10.53.

*4.3.3.2. EtCo(dThgH)$_2$Py (**3**).* Yield: 0.057 g (~57%). ^{1}H NMR (400 MHz, $CDCl_3$, δ ppm): Py_α = 8.69 (2H, d, J = 5.2 Hz), Py_β = 7.35 (2H, t, J = 7.0 Hz), Py_γ = 7.74 (1H, t, J = 8.0 Hz), thienyl protons = 7.49 (4H, d, J = 5.2 Hz), 6.98–6.96 (4H, m), 6.86 (4H, d, J = 3.2 Hz), 2.25 (2H, q, J = 7.6 Hz, $CoCH_2$), 0.59 (3H, t, J = 7.6 Hz), 18.87 (2H, s, O–H···O). ^{13}C NMR (125 MHz, $CDCl_3$, δ ppm): 149.90 (Py_α), 144.58 (C=N, C_q), 137.90 (Py_γ), 130.43, 129.49, 128.45, 126.09, 125.71, 29.79 (CH_2), 16.40 (CH_3). Anal. Calcd. for $C_{27}H_{24}CoN_5O_4S_4$: C, 48.42; H, 3.61; N, 10.46. Found: C, 48.24; H, 3.48; N, 10.62.

*4.3.3.3. n-PrCo(dThgH)$_2$Py (**4**).* Yield: 0.059 g (~58%). ^{1}H NMR (400 MHz, $CDCl_3$, δ ppm): Py_α = 8.68 (2H, d, J = 5.2 Hz), Py_β = 7.34 (2H, t, J = 6.8 Hz), Py_γ = 7.73 (1H, t, J = 8.0 Hz), thienyl protons = 7.49 (4H, d, J = 4.8 Hz), 6.97 (4H, t, J = 4.4 Hz), 6.86 (4H, d, J = 3.2 Hz), 2.12 (2H, t, J = 8.8 Hz, $CoCH_2$), 1.25–1.21 (2H, m), 0.84 (3H, t, J = 7.0 Hz), 18.88 (2H, s, O–H···O). ^{13}C NMR (125 MHz, $CDCl_3$, δ ppm): 149.83 (Py_α), 144.62 (C=N, C_q), 137.88 (Py_γ), 130.45, 129.47, 128.42, 126.07, 125.67, 37.43 ($CoCH_2$), 24.17 (CH_2), 14.85 (CH_3). Anal. Calcd. for $C_{28}H_{26}CoN_5O_4S_4$: C, 49.19; H, 3.83; N, 10.24. Found: C, 48.96; H, 3.64; N, 10.38.

Table 5
Crystal data and structure refinement details for **1**, **2**, **3**, **6** and **7**.

Parameters	**1**	**2**	**3**	**6**	**7**
Empirical formula	$C_{26}H_{21}Cl_3CoN_5O_4S$	$C_{26}H_{22}CoN_5O_4S_4$	$C_{27}H_{24}CoN_5O_4S_4$	$C_{32}H_{26}CoN_5O_4S_4$	$C_{34}H_{29.5}Cl_{4.5}CoN_5O_{6.5}S_4$
Formula weight	761.00	655.66	669.68	731.75	958.82
Temp (K)	100(2)	100(2)	100(2)	100(2)	100(2)
Crystal system	Orthorhombic	Monoclinic	Triclinic	Monoclinic	Triclinic
Space group	*Pbca*	*P*2$_1$/*c*	*P*-1	*P*2$_1$/*n*	*P*-1
Unit cell dimension					
a (Å)	17.500(5)	8.993(3)	9.382(3)	9.583(5)	9.733(3)
b (Å)	18.453(5)	10.865(4)	12.291(4)	31.288(5)	19.078(5)
c (Å)	19.250(5)	27.480(9)	14.223(5)	10.255(5)	23.497(7)
α (°)	90.000	90.000	115.377(5)	90.000(5)	111.042(5)
β (°)	90.000	94.415(6)	103.084(5)	90.820(5)	94.710(5)
γ (°)	90.000	90.000	95.893(6)	90.000(5)	102.981(5)
V (Å^3)	6216(3)	2677.3(15)	1406.2(8)	3074(2)	3903.8(18)
Z	8	4	2	4	4
ρ (calc), g/cm^3	1.626	1.627	1.582	1.581	1.631
μ (mm^{-1})	1.121	0.998	0.952	0.878	1.015
F (000)	3088	1344	688	1504	1952
Crystal size (mm^3)	0.35 × 0.26 × 0.18	0.32 × 0.21 × 0.16	0.53 × 0.34 × 0.22	0.41 × 0.33 × 0.22	0.51 × 0.36 × 0.23
Index ranges	$-23 \le h \le 18$	$-11 \le h \le 11$	$-11 \le h \le 11$	$-11 \le h \le 11$	$-11 \le h \le 11$
	$-17 \le k \le 24$	$-10 \le k \le 14$	$-14 \le k \le 14$	$-37 \le k \le 35$	$-15 \le k \le 22$
	$-25 \le l \le 25$	$-35 \le l \le 36$	$-13 \le l \le 17$	$-12 \le l \le 11$	$-27 \le l \le 25$
No. of rflns collected	39296	16976	7543	16372	20272
No. of indep rflns	7777	6598	5143	5706	13526
GOOF on F^2	1.104	1.085	1.131	1.055	1.035
Final *R* indices	R_1 = 0.0587	R_1 = 0.0630	R_1 = 0.0539	R_1 = 0.0527	R_1 = 0.0634
($I > 2\sigma(I)$)	wR_2 = 0.1392	wR_2 = 0.1569	wR_2 = 0.1414	wR_2 = 0.1272	wR_2 = 0.1602
R indices (all data)	R_1 = 0.0980	R_1 = 0.1073	R_1 = 0.0660	R_1 = 0.0734	R_1 = 0.0883
	wR_2 = 0.1898	wR_2 = 0.2262	wR_2 = 0.1657	wR_2 = 0.1424	wR_2 = 0.1999
Data/restraints/param	7777/46/412	6598/20/399	5143/10/386	5706/32/455	13526/52/1067

*4.3.3.4. n-BuCo(dThgH)$_2$Py (**5**).* Yield: 0.061 g (~60%). ^{1}H NMR (400 MHz, $CDCl_3$, δ ppm): Py_α = 8.69 (2H, d, J = 5.2 Hz), Py_β = 7.34 (2H, t, J = 6.8 Hz), Py_γ = 7.73 (1H, t, J = 7.6 Hz), thienyl protons = 7.48 (4H, d, J = 4.8 Hz), 6.98–6.96 (4H, m), 6.85 (4H, d, J = 3.2 Hz), 2.14 (2H, t, J = 8.6 Hz, $CoCH_2$), 1.30–1.24 (2H, m), 1.20–1.12 (2H, m), 0.80 (3H, t, J = 7.2 Hz), 18.87 (2H, s, O–H···O). ^{13}C NMR (125 MHz, $CDCl_3$, δ ppm): 149.85 (Py_α), 144.61 (C=N, C_q), 137.88 (Py_γ), 130.49, 129.44, 128.41, 126.09, 125.67, 34.87 ($CoCH_2$), 33.30 (CH_2), 23.56 (CH_2), 14.01 (CH_3). Anal. Calcd. for $C_{29}H_{28}CoN_5O_4S_4$: C, 49.92; H, 4.04; N, 10.04. Found: C, 50.03; H, 3.91; N, 10.15.

*4.3.3.5. BnCo(dThgH)$_2$Py (**6**).* Yield: 0.078 g (~72%). ^{1}H NMR (400 MHz, $CDCl_3$, δ ppm): Py_α = 8.64 (2H, d, J = 5.2 Hz), Py_β = 7.32 (2H, t, J = 7.0 Hz), Py_γ = 7.71 (1H, t, J = 7.8 Hz), thienyl/aromatic protons = 7.45 (4H, d, J = 5.2 Hz), 7.12–7.07 (3H, m), 6.94–6.91 (6H, m), 6.69 (4H, d, J = 3.6 Hz), 3.35 (2H, s, $CoCH_2$), 18.90 (2H, s, O–H···O). ^{13}C NMR (125 MHz, $CDCl_3$, δ ppm): 150.03 (Py_α), 144.75 (C=N, C_q), 137.95 (Py_γ), 130.37, 129.65, 129.00, 128.37, 128.24, 126.03, 125.71, 125.00, 34.61 (CH_2). Anal. Calcd. for $C_{32}H_{26}CoN_5O_4S_4$: C, 52.52; H, 3.58; N, 9.57. Found: C, 52.41; H, 3.55; N, 9.60.

*4.3.4. Synthesis of BnO$_2$Co(dThgH)$_2$Py (**7**)*

A solution of complex **6** (0.030 g, 0.041 mmol) in CH_2Cl_2 (10 mL) was irradiated with a 200 W tungsten lamp kept at a distance of approximately 10 cm, and pure oxygen gas was bubbled into this solution for 1 h at 0 °C. The solvent was evaporated under reduced pressure to obtain a crude product of complex **7**. The crude product was further purified on the silica gel column using 5% ethyl acetate/CH_2Cl_2. Yield: 0.026 g (~81%). ^{1}H NMR (400 MHz, $CDCl_3$, δ ppm): Py_α = 8.45 (2H, d, J = 5.2 Hz), Py_β = 7.21 (2H, t, J = 6.4 Hz), Py_γ = 7.63 (1H, t, J = 7.6 Hz), thienyl/aromatic protons = 7.44 (4H, d, J = 5.2 Hz), 7.03–6.96 (5H, m), 6.90–6.88 (4H, m), 6.79 (4H, d, J = 4.0 Hz), 4.32 (2H, s, O_2CH_2), 19.02 (2H, s, O–H···O). ^{13}C NMR (125 MHz, $CDCl_3$, δ ppm): 150.91 (Py_α), 146.75 (C=N, C_q), 138.72 (Py_γ), 136.56, 130.63, 130.10, 129.49, 129.05, 127.79, 127.40, 126.03, 125.85, 78.28 (O_2CH_2). Anal. Calcd. for $C_{32}H_{26}CoN_5O_6S_4$: C, 50.32; H, 3.43; N, 9.17. Found: C, 50.44, H, 3.48; N, 9.10.

Acknowledgments

We are thankful to the Department of Science and Technology (DST), Government of India and the Council of Scientific and Industrial Research (CSIR), India for financial support. K. K. thanks UGC, New Delhi, India for Senior Research Fellowship (SRF).

Appendix A. Supplementary material

CCDC 832464-832468 contain the supplementary crystallographic data for this paper. These data can be obtained free of charge from the Director, CCDC, 12 Union Road, Cambridge CB2 1EX, UK (fax +44-1223-336033; email: deposit@ccdc.cam.ac.uk or www: http://www.ccdc.cam.ac.uk/). Supplementary data associated with this article can be found in the online version.

Appendix. Supplementary material

Supplementary data related to this article can be found online at doi:10.1016/j.jorganchem.2011.08.035.

References

[1] N. Bresciani-Pahor, M. Forcolin, L.G. Marzilli, L. Randaccio, M.F. Summers, P.J. Toscano, Coord. Chem. Rev. 63 (1985) 1–125.
[2] L. Randaccio, N. Bresciani-Pahor, E. Zangrando, L.G. Marzilli, Chem. Soc. Rev. 18 (1989) 225–250.
[3] L. Randaccio, Comments Inorg. Chem. 21 (1999) 327–376.
[4] B.D. Gupta, S. Roy, Inorg. Chim. Acta 146 (1988) 209–221.
[5] P.J. Toscano, L.G. Marzilli, Prog. Inorg. Chem. 31 (1984) 105–204.
[6] G.N. Schrauzer, J. Kohnle, Chem. Ber 97 (1964) 3056–3064.
[7] G.N. Schrauzer, Inorg. Synth. 11 (1968) 61–69.
[8] G.N. Schrauzer, Angew. Chem. Int. Ed. Engl. 15 (1976) 417–426.
[9] A. Rockenbaur, M. Eyor, M. Kwielinsci, S. Tyrlik, Inorg. Chim. Acta 58 (1982) 237–242.
[10] S. Nemeth, L. Simandi, J. Mol. Catal. 14 (1982) 87–93.
[11] B. Giese, Radicals in Organic Synthesis: Formation of Carbon-Carbon Bonds. Pergamon Press, Oxford, U.K, 1986.
[12] I. Das, S. Chowdhury, K. Ravikumar, S. Roy, B.D. Gupta, J. Organomet. Chem. 532 (1997) 101–107.
[13] A.K. Ghosh, Y. Chen, Tetrahedron Lett. 36 (1995) 505–508.
[14] M.W. Wright, M.E. Welker, J. Org. Chem. 61 (1996) 133–141.
[15] B.D. Gupta, V. Singh, K. Qanungo, V. Vijaikanth, R.S. Sengar, J. Organomet. Chem. 582 (1999) 279–281 (and refs cited therein).
[16] T. Brown, A. Dronsfield, A. Jablonski, A.S. Wilkinson, Tetrahedron Lett. 37 (1996) 5413–5416.
[17] S. Roy, I. Das, K. Bhanuprakash, B.D. Gupta, Tetrahedron 50 (1994) 1847–1858.
[18] J.L. Gage, B.P. Branchaud, Tetrahedron Lett. 38 (1997) 7007–7010.
[19] K. Kumar, B.D. Gupta, J. Organomet. Chem. 696 (2011) 2280–2286.
[20] D. Dolphin (Ed.), B_{12}, Wiley & Sons, New York, 1982.
[21] R. Banerjee, Chemistry and Biochemistry of B_{12}. Wiley & Sons, Inc., N. Y., 1999.
[22] K.L. Brown, Chem. Rev. 105 (2005) 2075–2149.
[23] L. Randaccio, S. Geremia, E. Zangrando, C. Ebert, Inorg. Chem. 33 (1994) 4641–4650.
[24] P. Siega, L. Randaccio, P.A. Marzilli, L.G. Marzilli, Inorg. Chem. 45 (2006) 3359–3368.
[25] B.D. Gupta, K. Qanungo, Organomet. Chem. 543 (1997) 125–134.
[26] B.D. Gupta, V. Vijaikanth, V. Singh, J. Organomet. Chem. 570 (1998) 1–7.
[27] B.D. Gupta, K. Qanungo, T. Barclay, W. Cordes, J. Organomet. Chem. 560 (1998) 155–161.
[28] B.D. Gupta, R. Yamuna, V. Singh, U. Tiwari, Organometallics 22 (2003) 226–232.
[29] D. Mandal, B.D. Gupta, Organometallics 24 (2005) 1501–1510.
[30] G. Dutta, K. Kumar, B.D. Gupta, Organometallics 28 (2009) 3485–3491.
[31] K. Kumar, B.D. Gupta, J. Organomet. Chem. 696 (2011) 3343–3350.
[32] M. Bhuyan, M. Laskar, D. Mandal, B.D. Gupta, Organometallics 26 (2007) 3559–3567.
[33] K.A. Lance, K.A. Goldsby, D.H. Busch, Inorg. Chem. 29 (1990) 4537–4544.
[34] C. López, S. Alvarez, M. Font-Bardia, X. Solans, J. Organomet. Chem. 414 (1991) 245–259.
[35] C. López, S. Alvarez, X. Solans, M. Font-Bardia, Polyhedron 11 (1992) 1637–1646.
[36] P.J. Toscano, L. Lettko, E.J. Schermerhorn, J. Waechter, K. Shufon, S. Liu, E.V. Dikarev, J. Zubieta, Polyhedron 22 (2003) 2809–2820.
[37] $\Delta\delta(^{13}C_{C=N})$ value has been taken instead of $\delta(^{13}C_{C=N})$. This is to avoid the direct effect of substituent on δ(C=N) value.
[38] R.W. Schurko, R.E. Wasylishen, J. Phys. Chem. A 104 (2000) 3410–3420.
[39] C.M. Ellitott, E. Hershenhart, R.G. Finke, B.L. Smith, J. Am. Chem. Soc. 103 (1981) 5558–5566.
[40] V. Alexander, V.V. Ramanujam, Inorg. Chim. Acta 156 (1989) 125–137.
[41] E. Ngameni, J. Ngoune, A. Nassi, M.M. Belombe, R. Roux, Electrochim. Acta 41 (1996) 2571–2577.
[42] F. Asaro, R. Dreos, G. Nardin, G. Pellizer, S. Peressini, L. Randaccio, P. Siega, G. Trauzher, C. Tavagnacco, J. Organomet. Chem. 601 (2000) 114–125.
[43] G. Dutta, B.D. Gupta, J. Organomet. Chem. 696 (2011) 892–896.
[44] C. Giannotti, C. Fontaine, A. Chiaroni, C. Richie, J. Organomet. Chem. 113 (1976) 57–65.
[45] A. Chiarony, C. Pascard-Billy, Bull. Soc. Chim. Fr. (1973) 781–787.
[46] N.W. Alcock, B.T. Golding, S. Mwesigye-kibende, J. Chem. Soc. Dalton Trans. (1985) 1997–2000.
[47] C. Fontaine, K.N.V. Duong, C. Marienne, A. Gaudemer, C. Giannotti, J. Organomet. Chem. 38 (1972) 167–178.
[48] C. Marienne, C. Giannotti, A. Gaudemer, J. Organomet. Chem. 54 (1973) 281–290.
[49] J. Deniau, A. Gaudemer, J. Organomet. Chem. 191 (1980) C1–C2.
[50] M. Kijima, H. Yamashita, T. Sato, J. Organomet. Chem. 474 (1994) 177–182.
[51] B.D. Gupta, S. Roy, Inorg. Chim. Acta 108 (1985) 261–264.
[52] B.D. Gupta, M. Roy, I. Das, J. Organomet. Chem. 397 (1990) 219–230.
[53] G. Dutta, M. Laskar, B.D. Gupta, Organometallics 27 (2008) 3338–3345.
[54] D. Mandal, B.D. Gupta, Organometallics 26 (2007) 658–670.
[55] International Tables for X-ray Crystallography, vol. IV. Kynoch Press, Birmingham, England, 1974.
[56] Smart & SAINT Software Reference Manuals, Version 6.45. Bruker Analytical X-ray Systems, Inc., Madison, WI, 2003.
[57] G.M. Sheldrick, SADABS, Software for Empirical Absorption Correction, Ver. 2.05. University of Göttingen, Göttingen, Germany, 2002.
[58] XPREP, 5.1, Siemens Industrial Automation Inc., Madison, WI, 1995.
[59] G.M. Sheldrick, SHELXL97, Program for Crystal Structure Refinement. University of Göttingen, Göttingen, Germany, 2008.